

## Design and Synthesis of Disulfide-based Macrocycles and their Heavy Metal Ion Complexation and Self-assembly Studies

Ishanki Bhardwaj\*

Department of Chemistry, Sir PT Sarvajani College of Science, MTB College Campus, Surat, Gujarat, India

### ABSTRACT

A set of disulfide-based macrocycles C4-C8 with different spacer groups were synthesized. They possess complexing abilities toward heavy metal ions such as Hg<sup>2+</sup> and Cd<sup>2+</sup>. C4 showed specific binding toward Hg<sup>2+</sup>, while C6 exhibited binding toward Cd<sup>2+</sup>. Self-assembly analysis depicted their varied morphologies dependent on spacer moiety and internal molecular arrangement.

**Key words:** Macrocycle, Click reaction, Heavy metal sensors, Self-assembly, Vesicles.

### 1. INTRODUCTION

Macrocycles have always owned a special place due to their chemical diversity and usefulness in biochemical research. Cyclic molecules with a variety of backbones have been synthesized and utilized for several synthetic and biological purposes [1-6]. Macrocycles generally possess more rigidity as compared to their acyclic analogs. Macrocyclization has been recognized as an efficient way to restrict conformation and impart the unique self-assembling ability to generate diverse supramolecular assemblies [7-12]. The self-assembly of rigid macrocycles into well-defined nanostructures has been the subject of intense study in recent years, both for basic and applied research.

In general, rigid aromatic macrocycles can self-assemble into cylindrical micelles or spherical structures [13-15]. These supramolecular self-assemblies can be controlled or altered by varying the building blocks. The introduction of amino acids in the macrocycles can impart distinct self-assembling features since amide bonds can facilitate inter and intramolecular hydrogen bonding [16-20]. They are helpful in introducing in-depth structural control, as they form primary, secondary, tertiary, and quaternary structures.

Macrocycles designed with non-metallic centers can act as receptors for metals. Soft non-metals like sulfur can induce affinity toward heavy metals such as mercury, cadmium, lead, and silver. Heavy metal ions are considered dangerous as they can accumulate in the body through pollution and thus cause serious diseases like prenatal brain damage, cognitive disorders and Minamata diseases, even at low concentrations. Thus, designing molecules that can act as receptors for these ions and are helpful in eliminating them is an important area of concern [21-27].

### 2. EXPERIMENTAL SECTION

#### 2.1. UV-visible Titration Experiments

Stock solutions of compounds C4-C8 were prepared in spectroscopy grade chloroform/acetonitrile with concentration (10<sup>-4</sup>-100<sup>-5</sup> M). Solutions of metal salts were prepared in chloroform/acetonitrile with concentration (10<sup>-1</sup>-10<sup>-2</sup> M). The absorbance of blank compound solution and on gradual addition of cation salt was recorded using Shimadzu double beam UV-visible spectrophotometer model UV-2450.

#### 2.2. Calculation of Binding Constants and Stoichiometry

The binding constants were calculated by UV-visible titration experiments using the Benesi-Hildebrand plot as standardized for 1:1 stoichiometry. The stoichiometry of binding was calculated by Job's plot from UV-vis. absorbance data.

#### 2.3. Optical Microscopy

Around 3 mM solution of the sample in HPLC grade methanol/chloroform (1:1) was made and mounted on a glass slide. Samples were viewed using Nikon Eclipse TS100 optical microscope system.

#### 2.4. Transmission Electron Microscopy (TEM)

Around 3 mM solution of the sample in HPLC grade methanol/chloroform (1:1) was used for TEM. All the sample solutions were filtered through a nylon syringe filter (0.2 μm). About 2 μL aliquot of the sample solution was placed on a 200 mesh copper grid and stained with 0.2% wt. Phosphotungstate in water for 2 min. and dried in air. Samples were viewed using a Philips CM 12 TEM.

#### 2.5. Scanning Electron Microscopy (SEM)

Around 3-4 mM solution in 1:1 methanol/chloroform was prepared, and one drop of compound solution was put on glass coverslip, which was pasted on carbon tape mounted on a stub, dried at room temperature, and coated with ~ 10 nm of gold. Samples were analyzed using SEM ZEISS EVO 50 SEM.

#### 2.6. Atomic Force Microscopy (AFM)

Around 3.0-4.0 mM solution in 1:1 methanol/chloroform was prepared, and one drop of compound solution was put on the silicon

#### \*Corresponding author:

Ishanki Bhardwaj,

E-mail: [ib@ptsience.ac.in](mailto:ib@ptsience.ac.in)

ISSN NO: 2320-0898 (p); 2320-0928 (e)

DOI: 10.22607/IJACS.2023.1102005

Received: 25<sup>th</sup> March 2023;

Revised: 09<sup>th</sup> April 2023;

Accepted: 19<sup>th</sup> April 2023

wafer. Samples were analyzed using Dimension Icon AFM operating at tapping mode in air. Images were recorded in air at room temperature and data analysis was performed using nanoscope 5.31r software.

### 3. RESULTS AND DISCUSSION

#### 3.1. Design and Synthesis

We report here disulfide-based macrocycles **C4-C8** decked with varied spacer groups (Figure 1). The macrocycles were synthesized by Cu-catalyzed azide-alkyne dipolar cyclo-addition reaction. The design of the macrocycles is carried out such that a rigid macrocycle is built around aromatic units using disulfide and triazole units. The S-S linkage not only provided flexibility and preorganization properties to the molecules but also soft centers. Consequently, these scaffolds possess dual characteristics; tuned morphology and heavy metal binders.

3, 3'- Dithiobisbenzoic acid (**C1**) is converted into acid chloride derivative (**C2**) by reacting it with  $\text{SOCl}_2$ . **C2** is further reacted with propargyl alcohol to give di (prop-2-yn-1-yl) 3, 3'-disulfaneyldibenzoate, which acts as the dialkyne system **C3** (Scheme 1).

**C3** is further tethered to different aromatic and aliphatic spacers based on various diazides by click reaction to give macrocycles **C4-C8**. **C3** was reacted with 1, 1'-Biphediazide in the presence of Cu (I) under argon atmosphere to give **C4** (Scheme 2). Similarly, **C3** was reacted with *m*-xylylene diazide and 1, 6- Diazohexane to give **C5** and **C6**; **C7**, respectively (Scheme 2). The reaction of **C3** with diazidoacetic ester derivative of L-Cystine amino acid diester yielded **C8** (Scheme 2). Synthesis of **C8** was carried out using  $\text{CuSO}_4 \cdot 5\text{H}_2\text{O}$  in the presence of sodium ascorbate in the EtOH/Toluene/water (6:3:1) mixture as the procedure followed for the synthesis of other macrocycles gave very poor yield. **C4-C6** contains only one disulfide linkage, whereas **C7** and **C8** possess two disulfide linkages opposite to each other, which help to provide additional flexibility to the macrocycles. During the synthesis of **C4-C8**, we obtained residues along with the shown structures, which were found to be insoluble in most of the available solvents employed for spectral characterization. Therefore, they were not characterized. The residue **C7** obtained along with **C6** was soluble in dimethylsulphoxide and turned out to be a dimer of it.

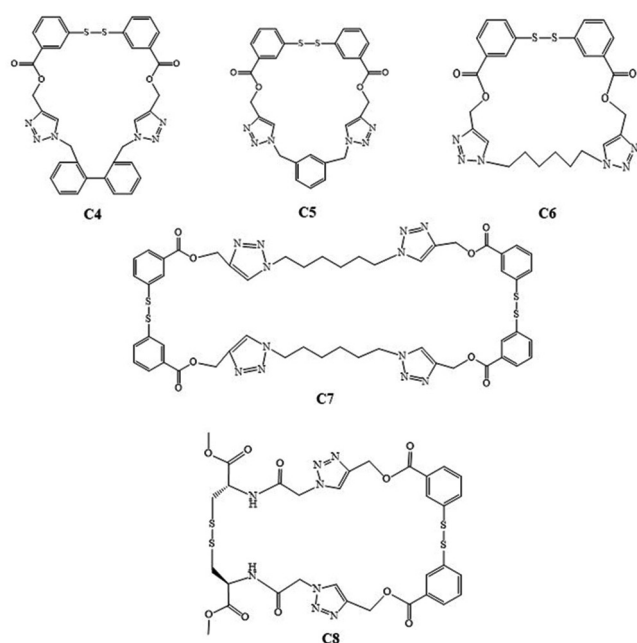
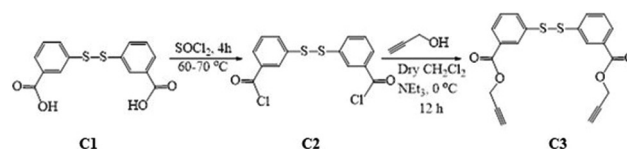


Figure 1: Structural representation of macrocycles **C4-C8**.

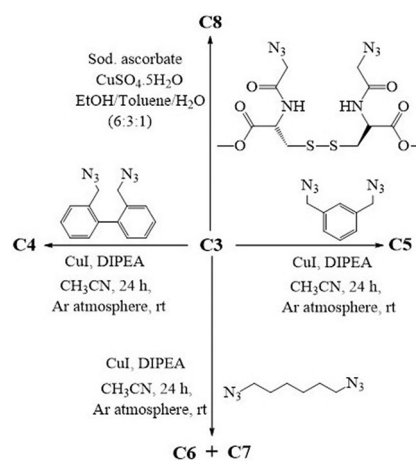
#### 3.2. Metal Ion Complexation Studies

As the macrocycles **C4-C8** contain non-metallic centers such as sulfur and oxygen, which can coordinate to metals and can form complex, we attempted to analyze the metal binding affinity of **C4-C8** toward metal ions such as  $\text{Hg}^{2+}$ ,  $\text{Pb}^{2+}$ ,  $\text{Ag}^+$ ,  $\text{Fe}^{2+}$ ,  $\text{Fe}^{3+}$ ,  $\text{Cd}^{2+}$ ,  $\text{Cu}^+$ ,  $\text{Mg}^{2+}$ ,  $\text{Ni}^{2+}$  and  $\text{Zn}^{2+}$  in 1:1  $\text{CH}_3\text{CN}/\text{CHCl}_3$ . The binding studies were carried out with perchlorate salts of metal ions. Binding affinity was evaluated by using UV-vis. spectroscopy titration experiments. UV-vis. titration profile of **C4** with  $\text{Hg}^{2+}$  showed a red shift in the absorbance peak at 240 nm upon slot-wise addition of metal salt (Figure 2a). The stoichiometry of binding as evaluated by Job's plot is 1:1 with  $\text{Hg}^{2+}$  (SI, Figure S1a). The binding constant as calculated by the Benesi-Hildebrand plot is  $2.7 \times 10^3 \text{ M}^{-1}$  (Inset Figure 2a). The specificity of binding of **C4** toward  $\text{Hg}^{2+}$  is also demonstrated by a UV-Vis. experiment, in which excess (117.0 equiv) of other metal perchlorate salts in the presence of 46.0 equiv of  $\text{Hg}(\text{ClO}_4)_2$  were added. The results showed negligible change in the absorbance of **C4** in the presence of other metal ions while it increases to  $\sim 3.8$  folds in the case of  $\text{Hg}(\text{ClO}_4)_2$ , which is a noteworthy observation (Figure 2b).

To investigate the possibility of involvement of pi-bonds of the aromatic/triazole ring in binding,  $^1\text{H}$ NMR titration experiment was performed by gradual addition of 0.0–40.0 equiv  $\text{Hg}(\text{ClO}_4)_2$  to **C4** in 1:1  $\text{CDCl}_3/\text{CD}_3\text{CN}$ . The studies revealed the negligible change in the chemical shift values of ring protons, thereby eliminating the existence of cation- $\pi$  interaction. Therefore, the mode of binding can be proposed as encapsulated mercuric ion inside **C4** with electrostatic interactions between sulphur/oxygen atoms and  $\text{Hg}^{2+}$  (Figure 3a). This binding model is supported by the observance of complex **C4** +  $\text{Hg}^{2+}$  +  $\text{ClO}_4^-$  in the form of white precipitates upon the addition of 40.0 equiv of  $\text{Hg}(\text{ClO}_4)_2$  salt to the 2 mM solution of **C4** (Figure 3b). It was confirmed by the presence of peak at  $m/z$  947.0896 in ESI-MS (SI, Figure S1b). The dried precipitate showed a melting point of 232–234°C, which is different from that of **C4**; 97–100°C. This kind of precipitation was not observed in the case of other cations. All these observations support the specific affinity of **C4** toward  $\text{Hg}^{2+}$ .



Scheme 1: Synthesis of dialkyne **C3**.



Scheme 2: Synthesis of macrocycles **C4-C8**.

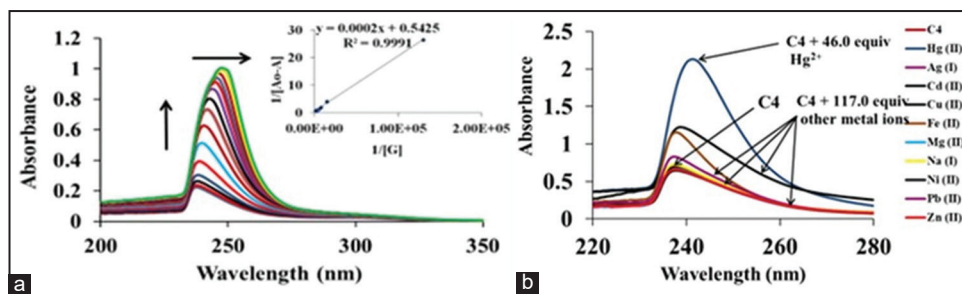


**Figure 2:** (a) UV-vis. titration profile of C4 ( $2.6 \times 10^{-5}$  M) with Hg ( $\text{ClO}_4$ )<sub>2</sub> ( $2.3 \times 10^{-2}$  M) (0–46 equiv) Inset: Benesi-Hildebrand plot of C4 with Hg<sup>2+</sup> (b) UV-vis. response of addition of all metal ions to C4 in 1:1 chloroform/acetonitrile (Other metal ions are added in excess {117.0 equiv} as compared to Hg<sup>2+</sup> ion).

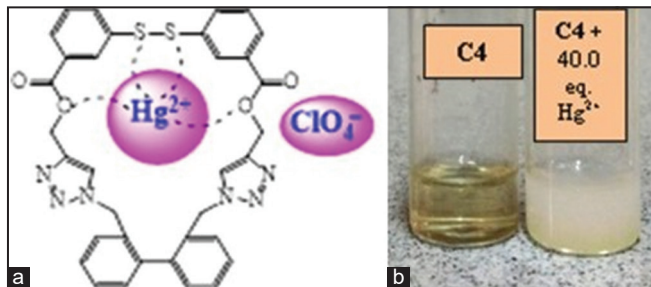


**Figure 3:** (a) Proposed binding mode of C4 with Hg<sup>2+</sup> and structure of complex (C4 + Hg<sup>2+</sup> + ClO<sub>4</sub><sup>-</sup>) (b) White precipitate observed upon addition of 40.0 equiv. of Hg ( $\text{ClO}_4$ )<sub>2</sub> ( $2.3 \times 10^{-3}$  M) to C4 ( $2.0 \times 10^{-3}$  M) in 1:1 chloroform/acetonitrile.

UV-vis. titration profile of C6 with Cd<sup>2+</sup> showed decrease in the absorbance at 240 nm upon slot-wise addition of metal salt (SI, Figure S2a). The Job's plot showed a 1:1 stoichiometry with Cd<sup>2+</sup> (SI, Figure S2b), and the Benesi-Hildebrand plot showed a binding constant of  $1.3 \times 10^3 \text{ M}^{-1}$  (SI, Figure S2c). The other macrocycles showed no significant binding toward Hg<sup>2+</sup>, Pb<sup>2+</sup>, Ag<sup>+</sup>, Fe<sup>2+</sup>, Fe<sup>3+</sup>, Cd<sup>2+</sup>, Cu<sup>+</sup>, Mg<sup>2+</sup>, Ni<sup>2+</sup> and Zn<sup>2+</sup> metal ions.

### 3.3. Self-assembly and Encapsulation Studies

As the designed macrocycles contain aromatic units, disulfide bridging and amino acid residue, this can impart unique morphological features to the molecules. Therefore, the self-assembling features of C4–C8 were analyzed in 1:1 CH<sub>3</sub>OH/CHCl<sub>3</sub> by using various microscopic techniques such as SEM, TEM, and AFM. The studies revealed the vesicular morphology of C4–C6, while C8 possessed flat bar-like morphology (Figure 4, SI, Figure S3a–e). These studies show the role of spacer groups in controlling morphology. Attaching amino acid spacer introduces additional hydrogen bonding ability and more flexibility to the molecule. The presence of two disulfide bridges in C8 might have changed the inter-spatial arrangement within the molecule and positioned it for linear self-assembly as compared to other macrocycles. Self-assembly analysis of C7 in dimethylsulphoxide and C3 in 1:1 CH<sub>3</sub>OH/CHCl<sub>3</sub> didn't show any specific morphology.

A closer look at the SEM images showed that the average size of vesicles formed from C4 and C5 is nearly same (200–400 nm), while the average size of vesicles of C6 increases to 3.0 μm (SI, Figure S4). The length of bars in the SEM image of C8 ranges from 9.2 μm–23 μm while the average width and height are 3.06 μm and 757 nm, respectively (SI, Figure S4).

After discovering the vesicular self-assembly of C4–C6, we moved our attention to evaluating the encapsulation potency of

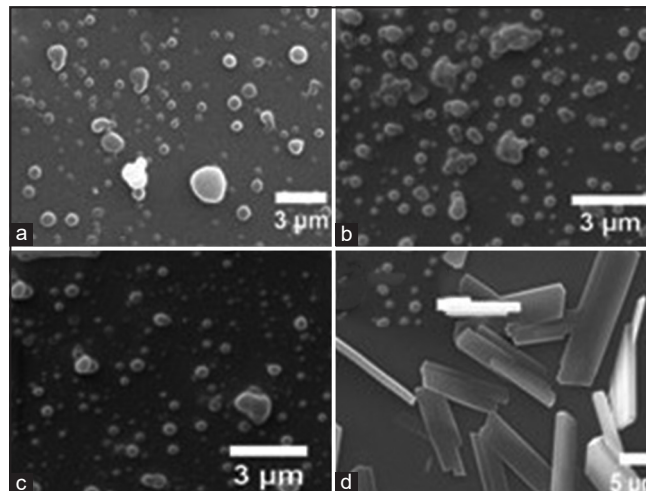


**Figure 4:** SEM images of macrocycle (a) C4 (3.1 mM) (b) C5 (2.8 mM) (c) C6 (2.96 mM) (d) C8 (2.8 mM) in 1:1 CHCl<sub>3</sub>/MeOH respectively.

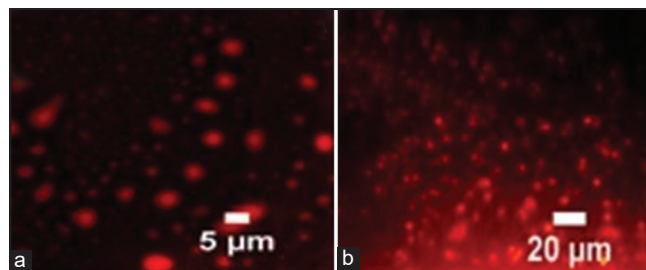


**Figure 5:** Fluorescence microscopic images ( $\lambda_{\text{ex}} = 510\text{--}560$  nm) of rhodamine B encapsulated (a) C4 (b) C5 1:1 CH<sub>3</sub>OH/CHCl<sub>3</sub>.

these vesicles. 0.02 equivalent of rhodamine B loaded vesicles appeared red ( $\lambda_{\text{max}} = 510\text{--}550$  nm) in case of C4 and C5, clearly indicating the encapsulation, while C6 doesn't showed encapsulation (Figure 5a and b). The most plausible reason for this is the presence of lesser number of aromatic units in C6 to interact with aromatic units in rhodamine B, yielding comparatively less stable interactions resulting in non-encapsulation.

## 4. CONCLUSION

In summary, we have synthesized disulfide-based macrocycles C4–C8 containing 1, 2, 3-triazole units. The complexing ability of C4–C8 toward metal ions was evaluated by UV-vis. spectroscopy. C4 showed binding toward Hg<sup>2+</sup> ion while C6 exhibited binding toward Cd<sup>2+</sup>. These macrocycles were demonstrated to show distinct

self-assembling features dependent upon the backbone moieties. C4-C6 showed vesicular self-assembly, while C8 showed flat bar-like morphology. This study shows that the positioning of aromatic moieties plays a distinct role in controlling self-assembly.

## 5. ACKNOWLEDGMENT

The author thanks CSIR, New Delhi, for the fellowship. The author acknowledges the Department of Textile Engineering and NRF, IITD for SEM, TEM, and AFM images.

## 6. SUPPLEMENTARY MATERIAL

Supplementary data (method of preparation, spectral data, and microscopic images) associated with this article can be found in the attached Word document.

## 7. REFERENCES

1. K. A. Yudin, (2015) Macrocycles: Lessons from the distant past, recent developments, and future directions, *Chemical Science*, **6**: 30-49.
2. E. Marsault, M. L. Peterson, (2011) Macrocycles are great cycles: Applications, opportunities, and challenges of synthetic macrocycles in drug discovery, *Journal of Medicinal Chemistry*, **54**: 1961-2004.
3. J. Huang, Y. Fang, W. Dehaen, (2020) Macrocyclic arenes functionalized with BODIPY: Rising stars among chemosensors and smart materials. *Chemosensors*, **8**: 51.
4. P. D. Sala, R. D. Regno, C. Talotta, A. Capobianco, N. Hickey, S. Geremia, M. D. Rosa, A. Spinella, A. Soriente, P. Neri, C. Gaeta, (2020) Prismarenes: A new class of macrocyclic hosts obtained by templation in a thermodynamically controlled synthesis, *Journal of American Chemical Society*, **142**: 1752-1756.
5. F. Yang, C. Liu, D. Yin, Y. Xu, M. Wuc, W. Wei, (2019) Atropisomer-based construction of macrocyclic hosts that selectively recognize tryptophan from standard amino acids, *Chemical Communications*, **55**: 14335-14338.
6. J. Yu, D. Qi, J. Li, (2020) Design, synthesis and applications of responsive macrocycles, *Communication Chemistry*, **3**: 189.
7. J. Yang, M. B. Dewal, D. Sobransingh, M. D. Smith, Y. Xu, L. S. Shimizu, (2009) Examination of the structural features that favor the columnar self-assembly of BIS-urea macrocycles, *Journal of Organic Chemistry*, **74**: 102-110.
8. Y. Yang, W. Feng, J. Hu, S. Zou, R. Gao, K. Yamato, M. Kline, Z. Cai, Y. Gao, Y. Wang, Y. Li, Y. Yang, L. Yuan, X. C. Zeng, B. Gong, (2011) Strong aggregation and directional assembly of aromatic oligoamide macrocycles, *Journal of American Chemical Society*, **133**: 18590-18593.
9. M. Kline, X. Wei, B. Gong, (2013) Aromatic oligoamide macrocycles with a backbone of reduced constraint, *Organic Letters*, **15**: 4762-4765.
10. S. R. Gagne, J. R. Neabo, M. Desroches, J. Larouche, J. Brisson, J. F. Morin, (2013) Topochemical polymerization of phenylacetylene macrocycles: A new strategy for the preparation of organic nanorods, *Journal of American Chemical Society*, **135**: 110-113.
11. H. J. Kim, Y. H. Jeong, E. Lee, M. Lee, (2009) Channel structures from self-assembled hexameric macrocycles in laterally grafted bent rod molecules, *Journal of American Chemical Society*, **131**: 17371-17375.
12. P. Lei, Q. Li, T. Meng, K. Deng, J. Wan, X. Xiao, Q. Zeng, (2022) Diverse self-assembly structures of a macrocycle revealed with STM by adjusting the solution concentration, *Chemistry-An Asian Journal*, **17**: e202101246.
13. S. R. Gagne, J. R. Neabo, M. Desroches, I. Levesque, M. Daigle, K. Cantin, J. F. Morin, (2013) Rigid organic nanotubes obtained from phenylene-butadiynylene macrocycles, *Chemical Communications*, **49**: 9546-9548.
14. J. K. Kim, E. Lee, M. C. Kim, E. Sim, M. Lee, (2009) Reversible transformation of helical coils and straight rods in cylindrical assembly of elliptical macrocycles, *Journal of American Chemical Society*, **131**: 17768-17770.
15. J. Montenegro, M. R. Ghadiri, J. R. Granza, (2013) Ion channel models based on self-assembling cyclic peptide nanotubes, *Accounts of Chemical Research*, **46**: 2955-2965.
16. X. Cheng, A. V. Heyen, W. Mamdouh, H. Uji-i, F. De Schryver, S. Hoger, S. De Feyter, (2007) Synthesis and adsorption of shape-persistent macrocycles containing polycyclic aromatic hydrocarbons in the rigid framework. *Langmuir*, **23**: 1281-1286.
17. R. J. Brea, C. Reiriz, J. R. Granja, (2010) Towards functional bionanomaterials based on self-assembling cyclic peptidnanotubes, *Chemical Society Reviews*, **39**: 1448-1456.
18. A. Ghorai, S. K. Reddy, B. Achari, P. Chattopadhyay, (2014) Rational construction of triazole/urea based peptidomimetic macrocycles as pseudocyclo- $\beta$ -peptides and studies on their chirality controlled self-assembly, *Organic Letters*, **16**: 3196-3199.
19. Z. Lin, Y. Yang, H. Zhan, Y. Hu, Z. Zhou, J. Zhu, Q. Wang, J. Deng, (2013) The self-assembly of cystine-bridged  $\gamma$ -peptide-based cyclic peptide-dendron hybrids, *Organic and Biomolecular Chemistry*, **11**: 8443-8451.
20. D. Ranganathan, V. Haridas, I. L. Karle, (1998) Cystinophanes, a novel family of aromatic-bridged cystine cyclic peptides: Synthesis, crystal structure, molecular recognition, and conformational studies, *Journal of American Chemical Society*, **120**: 2695-2702.
21. A. Jose, P. Nanjana, M. Porel, (2021) Sequence-defined oligomer as a modular platform for selective sub-picomolar detection and removal of  $Hg^{2+}$ , *Polymer Chemistry*, **12**: 5201-5208.
22. A Jose, R. Sahadevan, M. Vijay, S. Sadhukhan, M. Porel, (2023) Dansyl-appended sequence-defined oligomers for selective ultrasensitive detection of  $Hg^{2+}$  in water, paper strips, living cells and its efficient removal, *Sensors and Actuators B: Chemical*, **380**: 133335.
23. K. Ghosh, T. Sarkara, A. Samadder, (2012) A rhodamine appended tripodal receptor as a ratiometric probe for  $Hg^{2+}$  ions, *Organic and Biomolecular Chemistry*, **10**: 3236-3243.
24. J. M. Klein, V. Saggiomo, L. Reck, U. Luning, J. K. M. Sanders, (2012) Dynamic combinatorial libraries for the recognition of heavy metal ions, *Organic and Biomolecular Chemistry*, **10**: 60-66.
25. Y. Chen, J. Jiang, (2012) Porphyrin-based multi-signal chemosensors for  $Pb^{2+}$  and  $Cu^{2+}$ , *Organic and Biomolecular Chemistry*, **10**: 4782-4787.
26. Y. Pourghaz, P. Dongare, D. W. Thompson, Y. Zhao, (2011) Click functionalized poly (p-phenylene ethynylene) as highly selective and sensitive fluorescence turn-on chemosensors for  $Zn^{2+}$  and  $Cd^{2+}$  ions, *Chemical Communications*, **47**: 11014-11016.
27. L. Chen, Y. Cai, W. Feng, L. Yuan, (2019) Pillararenes as macrocyclic hosts: A rising star in metal ion separation, *Chemical Communications*, **55**: 7883-7898.

**\*Bibliographical Sketch**

Ishanki Bhardwaj is currently working as Adhyapak Sahayak in the Department of Chemistry, Sir PT Sarvajanik College of Science, Surat, Gujarat with an experience of more than 5 years. She qualified the CSIR-JRF with AIR-49 and GATE exam in 2010. She received her PhD degree in chemistry with specialization in bio-organic chemistry in 2016 from IIT Delhi. Her research interests include synthesis of bio-inspired molecules in supramolecular and biomimetics. She has also worked at various administrative levels along with academic duties. She has published papers in reputed international journals and attended seminars and conferences to present research work. She has guided four PG students for their dissertation work.